Nanostructure and Irreversible Colloidal Behavior of $Ca(OH)_2$: Implications in Cultural Heritage Conservation

C. Rodriguez-Navarro,*,† E. Ruiz-Agudo,† M. Ortega-Huertas,† and E. Hansen‡

Department Mineralogia y Petrologia, Universidad de Granada, Fuentenueva s/n, 18002 Granada, Spain, and The Getty Conservation Institute, 1400 Getty Center Dr., Suite 700, Los Angeles, California 90049-1684

Received May 19, 2005. In Final Form: September 9, 2005

Although $Ca(OH)_2$ is one of the oldest art and building material used by mankind, little is known about its nanostructural and colloidal characteristics that play a crucial role in its ultimate performance as a binder in lime mortars and plasters. In particular, it is unknown why hydrated lime putty behaves as an irreversible colloid once dried. Such effect dramatically affects the reactivity and rheology of hydrated lime dispersions. Here we show that the irreversible colloidal behavior of $Ca(OH)_2$ dispersions is the result of an oriented aggregation mechanism triggered by drying. Kinetic stability and particle size distribution analysis of oven-dried slaked lime or commercial dry hydrate dispersions exhibit a significant increase in settling speed and particle (cluster) size in comparison to slaked lime putty that has never been dried. Drying-related particle aggregation also leads to a significant reduction in surface area. Electron microscopy analyses show porous, randomly oriented, micron-sized clusters that are dominant in the dspersions both before and after drying. However, oriented aggregation of the primary $Ca(OH)_2$ nanocrystals (∼60 nm in size) is also observed. Oriented aggregation occurs both before and during drying, and although limited before drying, it is extensive during drying. Nanocrystals self-assemble in a crystallographically oriented manner either along the ⟨100⟩ or equivalent ⟨110⟩ directions, or along the $Ca(OH)_2$ basal planes, i.e., along [001]. While random aggregation appears to be reversible, oriented aggregation is not. The strong coherent bonding among oriented nanoparticles prevents disaggregation upon redispersion in water. The observed irreversible colloidal behavior associated with drying of $Ca(OH)_2$ dispersions has important implications in heritage conservation, particularly considering that nowadays hydrated lime is often the preferred alternative to portland cement in architectural heritage conservation. Finally, our study demonstrates that, fortuitously, hydrated lime could be one of the first nanomaterials used by mankind.

I. Introduction

Calcium hydroxide is an important chemical with numerous chemical, industrial, environmental, and architectural applications. It is used in hydrometallurgy, agriculture and soil conditioning, road stabilization, bleaching, sugar refinement, and acid mine drainage control.[1] Other examples of its applications include drinking water,[2] sewage sludge,[3] and wastewater[4] treatment; flue gas desulfuration;[5] pollutant emission control;[6] dentistry;[7] and as an additive in lubricating oil.[8] In addition, $Ca(OH)_2$ has been traditionally used as a primary material in architecture and decorative arts.[9,10] In all these applications, a high reactivity and superior rheological properties, both connected with a small (submicrometer) particle size, are of paramount importance.

$Ca(OH)_2$ is synthesized via either homogeneous or heterogeneous phase precipitation. Homogeneous phase precipitation normally takes place in the aqueous phase following mixing of strong base (e.g., NaOH) and Ca salt (e.g., $CaCl_2$ or $Ca(NO_3)_2$) solutions.[11,12] Variations to this route include synthesis in organic liquids (hydrocarbons) using surfactants that adopt a reverse-type micelle configuration around $Ca(OH)_2$ colloidal particles[8,13] and synthesis in water-in-oil emulsions.[14] Heterogeneous phase precipitation of $Ca(OH)_2$ occurs following hydration of CaO (quicklime), a process known as "lime slaking".[1] Addition of a stoichiometric amount of water (i.e., oxide: water mass ratio of 3.1) results in the formation of a dry powder made up of $Ca(OH)_2$ crystals (i.e., the so-called dry hydrate). A dry powder is desirable for both further processing (bagging) and reduction in transport costs, as water is added on site to make a putty for mortar preparation. If water is added in excess during hydration of CaO, a slaked lime putty develops.[10] The latter procedure for preparing hydrated lime putty, which is later mixed with an aggregate (usually quartz sand) in the preparation of lime plasters and mortars, has been known to mankind since the advent of pyrotechnology, ca. 10 000 B.C.[15,16] Slaked lime putty was the traditional

* Corresponding author. Tel: + 34 958 246616. Fax: + 34 958 243368. E-mail: carlosrn@ugr.es.

† Universidad de Granada.

‡ The Getty Conservation Institute.

(1) Boynton, R. S. *Chemistry and Technology of Lime and Limestone*; John Wiley & Sons: New York, 1980.

(2) Adroer, M.; Valero, F.; Poch, M.; Solà, C. *Ind. Eng. Chem. Res.* **1994**, *33*, 1501.

(3) Oppermann, B.; Mehlmann, M.; Peschen, N. *Zement-Kalk-Gips* **1991**, *44*, 265.

(4) Zhang, M.; Reardon, E. J. *Environ. Sci. Technol.* **2003**, *37*, 2947.

(5) Ho, C. S.; Shih, S. M.; Liu, C. F.; Chu, H. M.; Lee, C. D. *Ind. Eng. Chem. Res.* **2002**, *41*, 3357.

(6) Yan, K.; Chin, T.; Liang, D. T.; Laursen, K.; Ong, W. Y.; Yao, K.; Tay, J. H. *Environ. Sci. Technol.* **2003**, *37*, 2556.

(7) Murray, P. E.; Hafez, A. A.; Smith, A. J.; Cox, C. F. *Am. J. Dentistry* **2002**, *15*, 236.

(8) Born, M., Chive, A., Delfort, B. Colloidal Calcium Hydroxide, Its Preparation and Uses. U.S. Patent 5,756,432, 1995.

(9) Cowper, A. D. *Lime and Lime Mortars*; Building Research Station Special Report 9; Her Majesty Stationary Office: London, 1927.

(10) Elert, K.; Rodriguez-Navarro, C.; Sebastian, E.; Hansen, E.; Cazalla, O. *Studies Conservation* **2002**, *47*, 62.

(11) Klein, D. H.; Smith, M. D. *Talanta* **1968**, *15*, 229.

(12) Tadros, M. E.; Skalny, J.; Kalyoncu, R. S. *J. Colloid Interface Sci.* **1976**, *55*, 20.

(13) Delfort, B.; Born, M.; Chive, A.; Barre, L. *J. Colloid Interface Sci.* **1997**, *189*, 151.

(14) Nanni, A.; Dei, L. *Langmuir* **2003**, *19*, 933.

(15) Kingery, W. D.; Vandiver, P. B.; Prickett, M. *J. Field Archaeol.* **1988**, *14*, 219.

10.1021/la051338f CCC: $30.25
Published on Web 10/20/2005

preindustrial era material used, because excess water was needed to ensure complete hydration when using relatively inefficient manual slaking methods. Conversely, the dry hydrate is the standard product of the industrial hydration of lime.[1] Even though both processes lead to the production of calcium hydroxide, the physical−chemical properties of traditional slaked lime putty and commercial dry hydrated lime differ significantly.[1,17,18] In particular, the rheological properties (plasticity, workability, and dynamic viscosity) of slaked lime putty are superior to those of a putty prepared with dry hydrate.[19−22] Similarly, the reactivity of slaked lime putty appears to be higher than that of commercial dry hydrate putty.[23−25] On the other hand, traditional slaked lime putty undergoes a significant quality improvement upon long-term (months, or even years) storage under excess water.[24,26] Such a traditional "aging" procedure, which was known since Roman times, leads to both a significant particle size reduction and an increase in the amount of platelike particles.[26] As a result, the specific surface area of aged slaked lime putty increases,[26] its settling speed decreases,[17] and its rheological properties ameliorate.[20,22] However, aging of dry hydrate putty apparently does not result in any of the above-mentioned changes.[22]

Early studies in the first half of the 20th century tried to explain the differential behavior of slaked lime and dry hydrate putties, suggesting that hydrated lime behaved as an irreversible colloid.[1] Ray and Mathers observed that once hydrated lime putty is dried, it never fully regains its colloidal behavior when redispersed in water.[18] As a consequence, putties and mortars prepared with modern dry hydrated lime do not reach the high workability, fast carbonation, and early strength development of those prepared following traditional lime slaking procedures and subsequent mortar mixing.[24] Why this is so remains a mystery. Answering this question may have important scientific and technological implications, particularly in the field of architectural heritage conservation.

The colloidal behavior of homogeneous phase precipitated $Ca(OH)_2$ particles has been related to its nanophase nature.[27] However, little is known about the nature of colloidal particles developing during the most common, cost-effective, traditional way of preparing $Ca(OH)_2$, i.e., heterogeneous phase precipitation. It is well-known that colloids may undergo aggregation,[28] a process that strongly affects colloidal dispersions stability and rheological properties.[29] Considering that $Ca(OH)_2$ particles dispersed in water have an average ζ-potential of 34 mV,[30] the Derjaguin−Landau−Verwey−Overbeek (DLVO) theory for colloid stability[31] predicts that diffuse electrical double layer repulsive interactions would prevent aggregation, at least in diluted dispersions. However, slaked lime putties typically show high solids mass fractions (≥ 0.25),[32] and it has been known for decades that $Ca(OH)_2$ particles tend to form aggregates.[1,17] However, past studies[1,17] and recent analyses of $Ca(OH)_2$ particles, using N_2 adsorption (BET surface area) and scanning and transmission electron microscopy,[26,27,30] did not disclose how and to what extent $Ca(OH)_2$ particles aggregate.

According to Smoluchovski's model, agglomeration rates would peak during drying of $Ca(OH)_2$ dispersions. During the last stages of drying, agglomeration would be driven by capillary forces,[33] which eventually would overcome electrostatic repulsion. Ultimately, drying would mask any early aggregation, which further complicates the analysis of the aggregation process of $Ca(OH)_2$ particles. Attractive short-range van der Waals forces will keep particles attached once agglomeration has taken place. Since van der Waals forces are not insurmountable, it should be expected that redispersion of dry $Ca(OH)_2$ particles would allow them to regain their original colloidal behavior. However, they do not, even under vigorous stirring.[18] Recently it has been proposed that colloidal particles may assemble irreversibly via oriented (epitaxial) attachment.[34−36] Epitaxial assembly occurs when particles attach to each other in a crystallographically oriented fashion, thereby allowing interparticle structural continuity while energy is minimized.[37] Such bonding is very strong and may prevent separation of particles once they have attached. Although never observed in the $Ca(OH)_2$ system, oriented aggregation could help explain why $Ca(OH)_2$ particles do not fully regain their colloidal behavior once they have been dried and subsequently redispersed in water.

To better understand the colloidal behavior of heterogeneously precipitated $Ca(OH)_2$ and its irreversibility upon drying, we have studied the nanophase nature of hydrated lime. We show that the superior properties of slaked lime putty (if compared with dry hydrate putty) are connected with the presence of nanosized platelike $Ca(OH)_2$ particles. The irreversible colloidal behavior of hydrated lime is explained by an aggregation mechanism involving oriented (epitaxial) attachment of such nanosized $Ca(OH)_2$ crystals. To a limited extent, this process occurs in the dispersed phase. However, it is massive during drying. Such results are of relevance to the conservation of cultural heritage and suggest that slaked lime is one of the oldest nanomaterials known to mankind.

II. Experimental Section

II.1. Raw Materials and Preparation of Hydrated Lime Putties. Quicklime (CaO), designated "Graymont", for the preparation of slaked lime putty was obtained from Genlime and used as received. A commercial, dry hydrated Type N lime, designated "Chemstar Hydrate", was obtained from Chemicallime. The high calcium/low magnesium content of both materials was confirmed with ion chromatography (MgO content ranged

(16) Von Landsberg, D. *Zement-Kalk-Gips* **1992**, *45*, 199.
(17) Whitman, W. G.; Davis, G. H. B. *Ind. Eng. Chem.* **1926**, *18*, 118.
(18) Ray, K. W.; Mathers, F. C. *Ind. Eng. Chem.* **1928**, *20*, 475.
(19) Bonnell, D. G. R. *J. Soc. Chem. Ind.* **1934**, *53*, 279.
(20) Hansen, E.; Tagle, A.; Erder, E.; Baron, S.; Connell, S.; Rodriguez-Navarro, C.; van Balen, K. In *Proceedings of the International RILEM Workshop on Historic Mortars: Characterization and Tests*; Barton, P., Groot, C., Hughes, J. J., Eds.; RILEM Publication: Paris, 2000; p 197.
(21) Vávrová, P.; Kotlík, P. *Materiály Pro Stavbu* **2003**, *3*, 26.
(22) Atzeni, C.; Farci, A.; Floris, D.; Meloni, P. *J. Am. Ceram. Soc.* **2004**, *87*, 1764.
(23) Becker, H. *Chem. Ing. Tech.* **1987**, *59*, 228.
(24) Cazalla, O.; Rodriguez-Navarro, C.; Sebastian, E.; Cultrone, G.; De la Torre, M. J. *J. Am. Ceram. Soc.* **2000**, *83*, 1070.
(25) Rodriguez-Navarro, C.; Cazalla, O.; Elert, K.; Sebastian, E. *Proc. R. Soc. London Ser. A* **2002**, *458*, 2261.
(26) Rodriguez-Navarro, C.; Hansen, E.; Ginell, W. S. *J. Am. Ceram. Soc.* **1998**, *81*, 3032.
(27) Ambrosi, M.; Dei, L.; Giorgi, R.; Neto, C.; Baglioni, P. *Langmuir* **2001**, *17*, 4251.
(28) Lin, M. Y.; Lindsay, H. M.; Weitz, D. A.; Ball, R. C.; Klein, R.; Meakin, P. *Nature* **1989**, *339*, 360.
(29) Goodwin, J. W. In *Colloid Science*; Everett, D. H., Ed.; The Chemical Society: London, 1975; Vol. 2, Chapter 7; p 246.
(30) Giorgi, R.; Dei, L.; Ceccato, M.; Schettino, C.; Baglioni, P. *Langmuir* **2002**, *18*, 8198.
(31) Ottewill, R. H. In *Colloid Science*; Everett, D. H., Ed.; The Chemical Society: London, 1973; Vol. 1, Chapter 5, p 173.
(32) Hansen, E.; van Balen, K.; Rodriguez-Navarro, C. *2005 International Building Lime Symposium Proceedings*; National Lime Association: Washington DC, 2005.
(33) Scherer, G. W. *J. Am. Ceram. Soc.* **1990**, *73*, 3.
(34) Penn, R. L.; Banfield, J. F. *Science* **1998**, *281*, 969.
(35) Penn, R. L.; Banfield, J. F. *Geochim. Cosmochim. Acta* **1999**, *63*, 1549.
(36) Penn, R. L.; Oskam, G.; Strathamann, T. J.; Searson, P. C.; Stone, A. T.; Veblen, D. R. *J. Phys. Chem. B* **2001**, *105*, 2177.
(37) Penn, R. L. *J. Phys. Chem. B* **2004**, *108*, 12707.

from 0.2 to 0.6 wt %). The "hot" Graymont calcium oxide, as indicated by the ASTM C110 Reactivity Test,[38] was slaked with vigorous stirring in an initial mass ratio of 1:3 quicklime to water. Such proportion is recommended in the literature.[39] Slaked lime putty dispersions have an average solids mass fraction, ϕ, of 0.25, once supernatant solution was decanted. Such a ϕ value is typical for freshly slaked limes.[32] The lime putty made from the commercial dry hydrated lime was prepared with a similar ϕ. A fraction of each putty was oven-dried at 110 °C for 24 h, let to cool at room temperature, and subsequently redispersed in water (up to $\phi = 0.25$). Deionized water (water resistance less than 55 μS cm^{-1}) was used throughout. Putties were stored in covered containers under excess water throughout the length of testing. Right before testing, excess water was decanted. To avoid carbonation during storage and testing, containers were flushed with N_2 before airtight capping.

II.2. Kinetic Stability of $Ca(OH)_2$ Dispersions. Three batches of lime putty samples were prepared: (a) slaked lime putty; (b) slaked lime putty, first oven dried and subsequently redispersed in water; and (c) commercial dry hydrate lime dispersed in water. A 0.25-mL portion of each putty (with $\phi = 0.25$) was dispersed in 12 mL of saturated $Ca(OH)_2$ aqueous solution (i.e., $\phi = 0.02$) and vigorously stirred at room temperature. The relative kinetic stability of the dispersions has been calculated from the ratio of the optical densities of the supernatant liquid (i.e., saturated $Ca(OH)_2$ solution) and of the original dispersion determined at 600 nm (UV−vis spectrophotometer, Thermo Spectronic UNICAM UV 300), following the procedure outlined by Ambrosi et al.[27]

II.3. Characterization of $Ca(OH)_2$ Particles. The particle size distribution (PSD) of $Ca(OH)_2$ dispersions was measured using a Coulter LS 230 laser diffraction particle size analyzer. Prior to measurement, saturated $Ca(OH)_2$ aqueous solution was added to slaked lime putty or dry hydrate putty samples till $\phi = 0.1$ was reached. Such a ϕ value was selected because higher (0.25) or lower (0.02) values did not yield reproducible PSD results.

For the rest of the analyses (see below), putty samples were dried in an oven at 110 °C for 24 h. Dry hydrate lime samples were analyzed before and after putty preparation. Additionally, and to limit particle aggregation during drying, a set of putty samples were freeze-dried using a Labconco Lyph-Lock 6 apparatus. Samples were analyzed right after complete drying. Analysis of the shape, size and ultrastructure of particles was performed by means of field emission scanning electron microscopy (FESEM) using a Leo Gemini 1530 and transmission electron microscopy (TEM) using a Philips CM20, operated at a 200 kV acceleration voltage. For FESEM analysis, powder samples were placed onto carbon-coated sticky stubs before carbon coating. Prior to TEM observations, $Ca(OH)_2$ particles were dispersed in ethanol, sonicated 15 s, and deposited on carbon-coated copper grids. TEM observations were performed using a 40 μm objective aperture, which is a compromise between amplitude and phase contrast images. Lattice images with $d_{hkl} > 0.2$ nm were collected in this way. Selected area electron diffraction (SAED) images were collected using a 10 μm objective aperture. Such aperture allows collection of diffraction data from a circular area of 0.5 μm diameter. The crystal structure of the solids was checked by X-ray diffractometry (XRD) using a Philips PW-1710 diffractometer with an automatic slit. Measurement parameters were as follows: Cu Kα radiation ($\lambda = 1.5405$ Å), an exploration range from 10° to 70° 2θ, steps of 0.028° 2θ, and a goniometer speed of 0.01° 2θ s^{-1}. Crystallinity or "crystallite size", D_{hkl}, (i.e., coherent X-ray scattering domains), of $Ca(OH)_2$ was calculated using the Warren modification of the Scherrer equation[40]

$$D_{khl} = \frac{K\lambda}{\beta \cos \theta} \quad (1)$$

where K is the crystallite-shape factor (0.94 for 00l reflections and 1.84 for the h00 or hk0 ones, respectively),[41] λ is the X-ray wavelength, β is the X-ray diffraction broadening (i.e., Bragg peak full width at half-maximum: fwhm, in radians), and θ is the Bragg angle. XRD data collection and peak broadening analysis was performed using the XPowder software package,[42] which included instrumental broadening correction.

The N_2 sorption isotherms were obtained at 77 K on a Micromeritics Tristar 3000 under continuous adsorption conditions. Prior to measurement, powder samples were heated at 200 °C for 2 h and outgassed to 10^{-3} Torr using a Micromeritics Flowprep. BET analysis[43] was used to determine the total specific surface area (SSA). The total pore volume (V_{total}) and micropore volume (V_{micro}) of the samples were calculated using t-plot analysis.[44,45] The BJH method[46] was used to obtain pore size distribution curves.

The degree of agglomeration D_{BET}/D_{hkl} was obtained from the average particle size, D_{BET}, determined from the specific surface area, and from the crystallite size D_{100}, determined by means of XRD.[47] An aspect ratio of 2.5 (i.e., D_{100}/D_{001}) was considered for D_{BET} calculation of $Ca(OH)_2$ hexagonal plates, a value consistent with XRD, FESEM, and TEM results (see the following section).

Table 1. Properties of $Ca(OH)_2$ Particles

property	slaked lime	dry hydrate
dispersion stability (100 × optical density/min)	1.63 ± 0.4 5.13 ± 0.5[a]	4.84 ± 0.4
BET surface area (m^2 g^{-1})		
freeze-dried	27.8 ± 0.8	–
dried	21.7 ± 2.3	19.5 ± 0.9[b]
dried + redispersed + dried	20.8 ± 0.7	17.9 ± 1.2[c]
dried + redispersed + freeze-dried	23.5 ± 0.3	26.8 ± 0.2[c]
total pore volume (cm^3 g^{-1})	0.1963 ± 0.02	0.1447 ± 0.02
micropore volume (cm^3 g^{-1} STP)	0.0009 ± 0.0002	0.0006 ± 0.0001
D_{hkl} (nm)		
D_{001}	26 ± 5	20 ± 2
D_{100}	63 ± 13	51 ± 7
D_{110}	63 ± 10	55 ± 2
D_{BET} (nm)		
freeze-dried	144	149[c]
dried	185	206[b]
D_{BET}/D_{100}		
freeze-dried	2.29	2.92
dried	2.93	4.03

[a] Following drying and redispersion. [b] Original dry powder. [c] Original dry powder dispersed in water and then dried or freeze-dried.

III. Results and Discussion

III.1. Kinetic Stability and Particle Size Distribution. A significant increase in the settling speed of slaked lime was observed following oven-drying and redispersion in water. Such an increase was indicated by a fall of turbidity at faster rates than in the case of the original slaked lime putty. The absolute value of the initial (first 5 min) slope of the absorbance vs time curve was almost 3 times higher than that of the original slaked lime putty (Table 1). Such a slope value is slightly higher than that of the dispersion prepared with the commercial dry hydrate lime. These results are in agreement with early

(38) ASTM C 110-95b *Standard Test Methods for Physical Testing of Quicklime, Hydrated, and Limestone*; American Society for Testing and Materials: Philadelphia, PA.
(39) Lordley, H. E. Water Seawage Works, Reference Data R-214, 1955.
(40) Klug, H. P.; Alexander, L. E. *X-ray Diffraction Procedures*, 2nd ed.; Wiley: New York, 1974; Chapter 9.
(41) Meyer, M.; Bée, A.; Talbot, D.; Cabuil, V., Boyer, J. M.; Réppetti, B.; Garrigos, R. *J. Colloid Interface Sci.* **2004**, *277*, 309.
(42) Martín-Ramos, J. D. *XPowder: A Software Package for Powder X-ray Diffraction Analysis, Version 2004.03*, 2004 [www.xpowder.com].
(43) Brunauer, S.; Emmett, P. H.; Teller, E. *J. Am. Chem. Soc.* **1938**, *60*, 309.
(44) Gregg, S. J.; Sing, K. S. W. *Adsorption, Surface Area and Porosity*, 2nd ed.; Academic Press: London, 1982.
(45) Adamson, R. W.; Gast, A. P. *Physical Chemistry of Surfaces*, 6th ed.; Wiley: New York, 1997; Chapter 17.
(46) Barrett, E. P.; Joyner, L. S.; Halenda, P. P. *J. Am. Chem. Soc.* **1951**, *73*, 373.
(47) Alvarado, E.; Torres-Martinez, L. M.; Fuentes, A. F.; Quintana, P. *Polyhedron* **2000**, *19*, 2345.

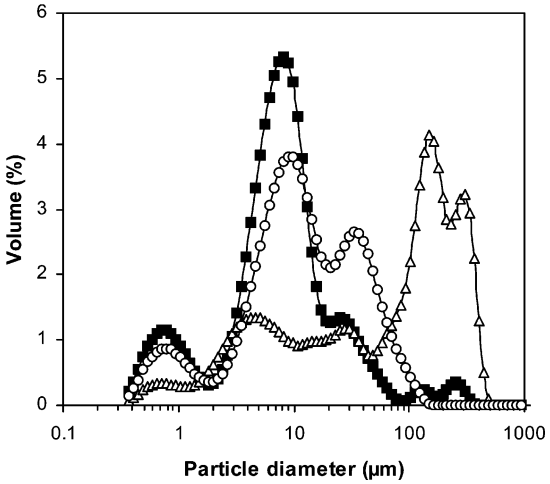

Figure 1. Particle size distribution of (■) slaked lime putty, (△) oven-dried slaked lime putty, and (○) commercial dry hydrate lime putty.

studies showing that the traditionally slaked limes settle more slowly than the suspensions made from commercial dry hydrate.[48]

The PSD of all tested hydrated lime samples was polymodal (Figure 1), which is typical for calcium hydroxide particles precipitated via heterogeneous phase reaction.[49] Arai[49] reported that (nearly) monodisperse $Ca(OH)_2$ particles are obtained via heterogeneous phase precipitation, while lime slaking leads to the formation of irregularly shaped particles of very fine aggregated crystals of $Ca(OH)_2$ with sizes of the order of 1 μm.

A significant change in PSD occurred following drying and redispersion of the slaked lime putty (Figure 1). Mean particle (i.e., cluster or aggregate) size increased from 7 $\pm$ 3 up to 47 $\pm$ 6 μm. A significant reduction in the amount of particles with sizes <1 μm and $\sim$10 μm was observed. The PSD of the dry hydrate putty fell between that of the original slaked lime putty and that of the oven-dried/redispersed slaked lime putty. The dry hydrate putty had larger aggregates (mean particle size of 11 $\pm$ 3 μm) than the original slaked lime. It showed a polymodal PSD with maxima at ca. 0.7, 10, and 13 μm. Clusters with size <1 μm were slightly less abundant. Note that the "particle" size determined using the laser diffraction apparatus does not refer to the size of the individual $Ca(OH)_2$ crystals; rather, it refers to the size of clusters or aggregates (see FESEM and TEM results in the following paragraphs).

Overall, kinetic stability and PSD results point to a general increase in particle (cluster) size following drying, resulting from either the original industrial process producing the dry hydrate or the drying of traditionally slaked lime putty. In the latter case, the change is much more significant. Kinetic stability results are consistent with PSD. This means that the Stokes law for sedimentation rate, which states a dependence of the settling rate on the square of the particle radius,[50] applies in our case.

III.2. N_2 Sorption Analyses. Representative N_2 adsorption isotherms of $Ca(OH)_2$ samples are shown in Figure 2a. Isotherms were of type II[51] and reflect the

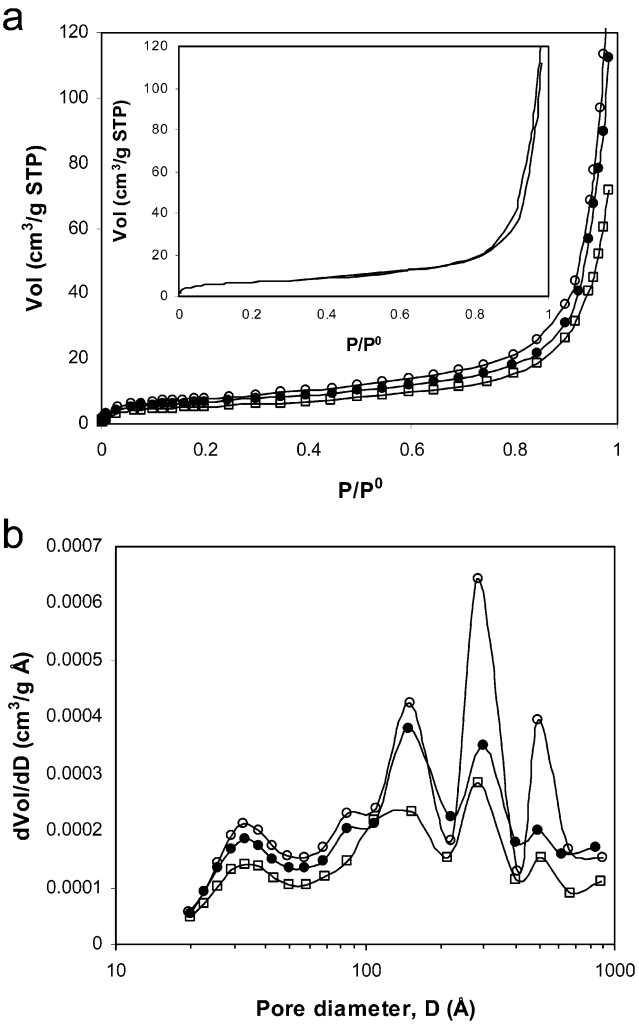

Figure 2. N_2 sorption analysis of $Ca(OH)_2$: (a) adsorption isotherms and (b) BJH pore size distribution plots. The inset in part a shows a typical $Ca(OH)_2$ adsorption−desorption isotherm with a H_3 hysteresis loop. Symbols: (○) freeze-dried slaked lime putty, (●) oven-dried slaked lime putty, and (□) commercial dry hydrate lime putty.

nonporous nature of the solids.[44] Besides the slightly higher slope of freeze-dried slaked lime at $P/P^0 < 0.1$, no significant variations in isotherm shape were observed among the different samples tested. Additionally, all isotherms showed a large type H_3 hysteresis loop (inset in Figure 2a), which did not exhibit any limiting adsorption at high P/P^0. Such a hysteresis loop is typical of aggregates of platelike particles giving rise to slit-shaped pores.[52] BJH pore size distribution plots show that all samples had mesoscale pores (Figure 2b). Note that in all cases the total pore volume was very low, while the micropore volume was negligible (Table 1). Both oven-dried and freeze-dried slaked lime putty samples had slightly higher amounts of mesopores (pore diameters ranging from 20 to 500 Å) than the dry hydrate. A similar behavior was observed in the case of the macropore (pore diameters greater than 500 Å) size distribution. Overall, pore size distribution results are consistent with the (slightly) lower SSA of the dry hydrate (Table 1). Sorption analyses are in agreement with PSD results, inasmuch as a lower SSA is expected in the dry hydrated lime, since it has coarser particles (clusters) than the slaked lime.

(48) Holmes, M. E.; Fink, G. J.; Mathers, F. C. *Chem. Metall. Eng.* **1922**, *27*, 1212.
(49) Arai, Y. *Chemistry of Powder Production*; Chapman & Hall: London, 1996; Chapter 4.
(50) Kissa, E. *Dispersions. Characterization, Testing, and Measurement*; Surfactants Science Series; Marcel Dekker Inc.: New York, 1999; Chapter 9, Vol. 84.
(51) Brunauer, S. *The Adsorption of Gases and Vapors*, Princeton University Press: Princeton, NJ, 1945; Vol. 1.
(52) Yu, J. C.; Xu, A.; Zhang, L.; Song, R.; Wu, L. *J. Phys. Chem. B* **2004**, *108*, 64.

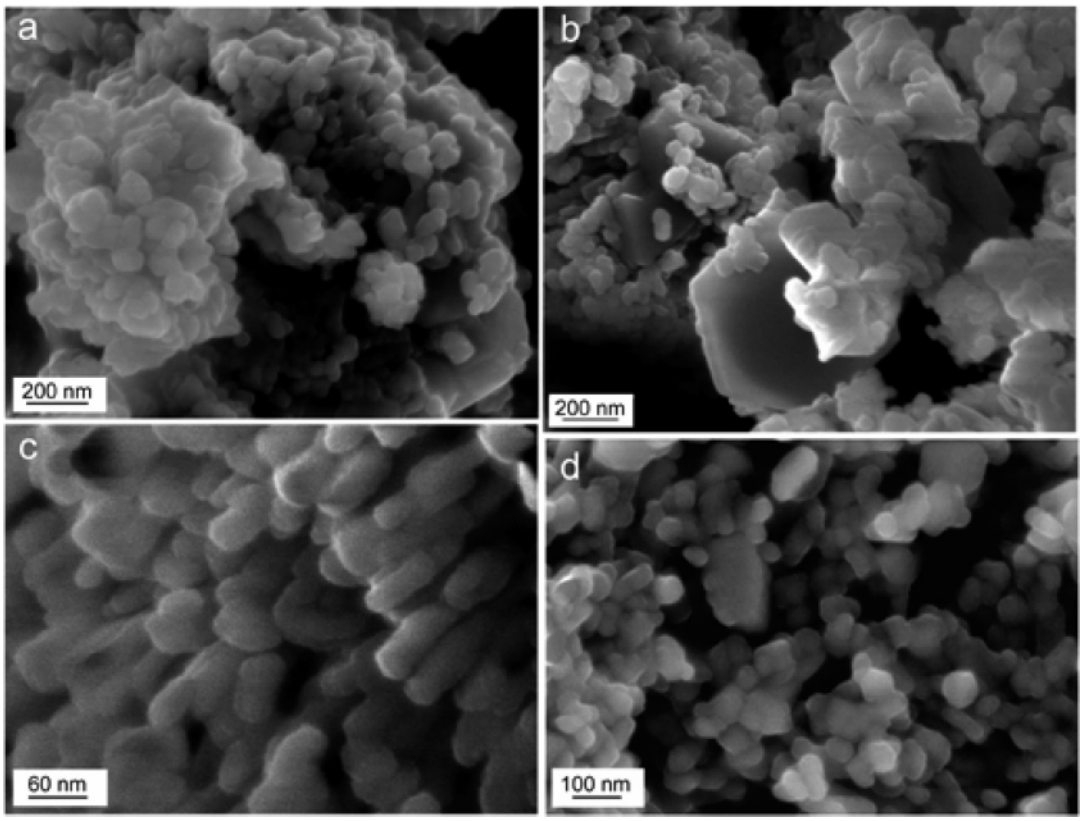

Figure 3. FESEM photomicrographs of (a) oven dried slaked lime putty showing agglomeration of platelike $Ca(OH)_2$ nanocrystals and (b) commercial dry hydrated lime, also displaying extensive agglomeration. In both parts a and b, randomly oriented and crystallographically oriented aggregates are present. (c) Detail of a representative oriented aggregate of $Ca(OH)_2$ nanoparticles attached by the (0001) planes and (d) randomly oriented aggregates in freeze-dried slaked lime samples.

A significant reduction in SSA occurred following drying of the lime putties, subsequent redispersion in water, and final oven-drying (Table 1). This effect was additive; i.e., a further reduction in SSA was observed upon a second redispersion and oven-drying. Considering that the solubility of $Ca(OH)_2$ at 20 °C is 0.165 g/100 g of saturated solution,[1] it could be argued that such SSA reduction is due to preferential dissolution of the smaller particles—those that most significantly contribute to the overall SSA—once redispersed in water. To determine if that effect was at work here, a set of samples was redispersed in saturated $Ca(OH)_2$ solution before drying and surface area measurement. However, SSA values for the latter samples were similar to those of the samples dispersed in deionized water. These results evidence that water, i.e., the standard liquid used for the preparation of a lime putty, does not alter the surface area (or the overall PSD) of a putty. This is most probably due to the high solid content of the putties. Instead, the observed SSA reduction can be explained by taking into account that drying induces particle coalescence and increases particle (cluster) size, as evidenced by both kinetic stability and PSD results.

Freeze-dried samples had SSA values ~22% higher than those of oven-dried samples (Table 1). Apparently, freeze-drying limits agglomeration, yielding a more accurate picture of the SSA of the particles in the original dispersions. These results point to drying of hydrated lime putty as the ruling mechanism leading to particle agglomeration and SSA reduction. Interestingly, a reduction in SSA values was also observed in oven-dried samples following redispersion and ulterior freeze-drying (Table 1). The latter values fell between those of the original freeze-dried and oven-dried samples. This implies that standard drying leads to both reversible and irreversible aggregation of colloidal $Ca(OH)_2$ particles. While a fraction of the clusters formed during drying disaggregate upon redispersion, another fraction does not. That is why the SSA of the lime putty that was oven-dried, redispersed, and freeze-dried was still higher than that of the original oven-dried putty but did not regain the values of the original freeze-dried putty. This trend is observed in the case of both the slaked lime putty and the putty prepared with the commercial dry hydrate lime (Table 1). Note, however, that in the latter case no data could be obtained regarding the SSA of freeze-dried putty not subjected to previous drying, since the industrial process of lime hydration results in a dry powder.

III.3. Nano- and Microstructure of $Ca(OH)_2$ Particles and Aggregates. FESEM observations show the systematic presence of platelike nanoparticles that aggregate into micron-sized clusters. Typically, the size of individual $Ca(OH)_2$ particles ranged from 30 up to 200 nm (measured along the ⟨100⟩ or equivalent ⟨110⟩ directions). However, scarce micron-sized (1−3 μm) platelike particles were also observed. The nanosized, platelike crystals are very similar to those obtained via homogeneous phase precipitation under highly supersaturated conditions.[49]

No significant differences in morphology and size between oven-dried slaked lime and commercial dry hydrate particles were detected. In both cases randomly oriented aggregates were dominant (Figure 3a,b). However, numerous crystallographically oriented aggregates were observed in dry hydrate samples. These aggregates were characterized by nanoparticles that attach to each other by the basal (0001) planes (Figure 3c). Such attachment was rarely observed in freeze-dried slaked lime, where nonoriented aggregation was extensive (Fig-

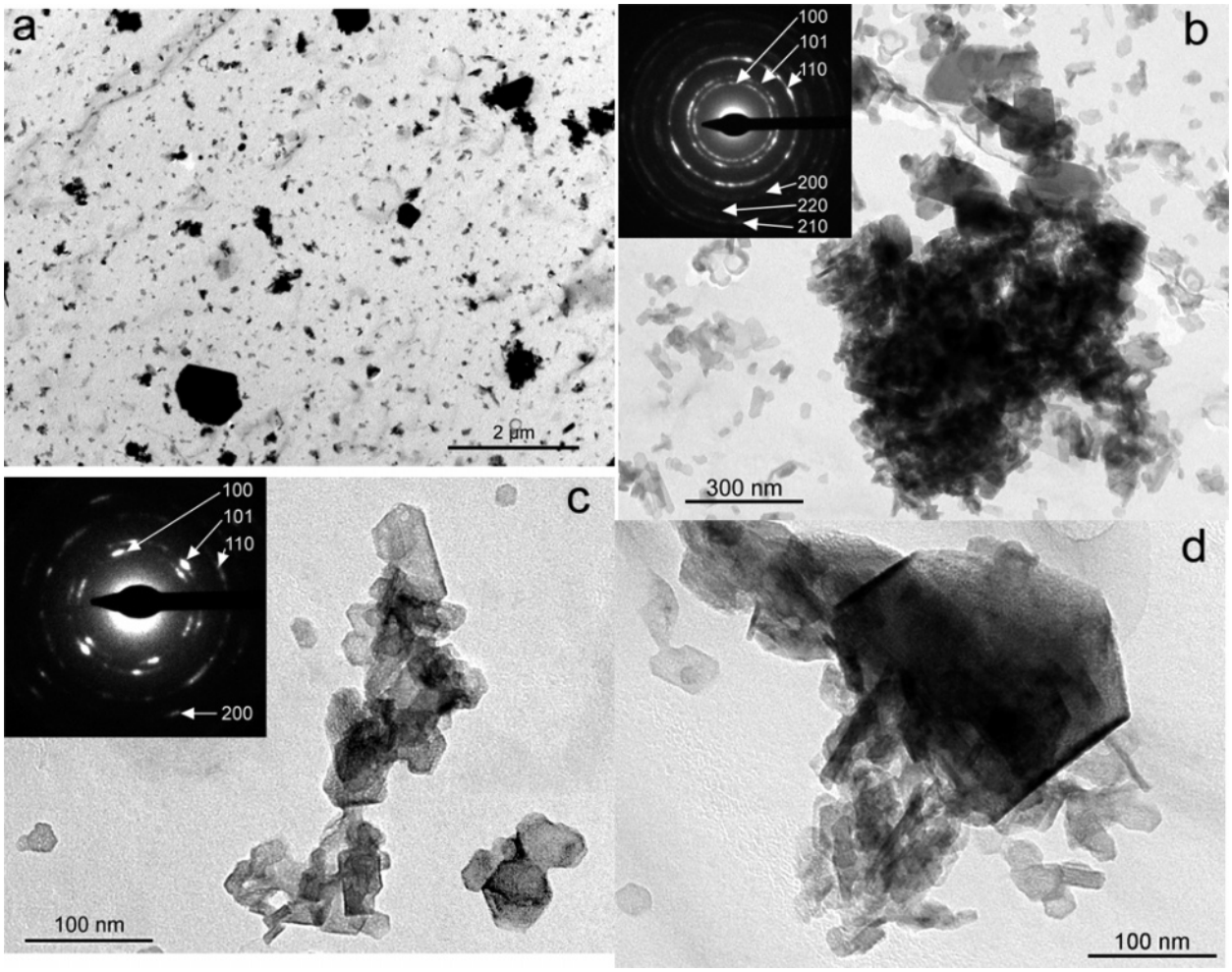

Figure 4. TEM photomicrographs of freeze-dried slaked lime: (a) low-magnification image showing different aggregates with sizes up to a few micrometers and (b) detail of a typical disoriented aggregate of numerous platelike crystals. The diffraction rings in the SAED pattern (inset, which includes *hkl* values of the Debye rings) evidence that the cluster is formed by randomly oriented $Ca(OH)_2$ crystals. (c) Oriented aggregates of a few nanocrystals. The [001] zone axis SAED pattern (inset) confirms the crystallographic orientation of the nanocrystals in the (larger) aggregate; i.e., the SAED pattern of the aggregate is similar to that of a single crystal oriented along [001]. Note, however, the presence of discrete 101 diffraction spots due to a few nonoriented crystals located at the bottom of the image. (d) Isolated, large hexagonal platelike crystal surrounded by randomly oriented aggregates of nanocrystals.

ure 3d). Such observations point to two different aggregation mechanisms undergone by $Ca(OH)_2$ nanoparticles: nonoriented and oriented aggregation. While the former appears to operate both before and during drying, the latter appears to be triggered by drying of the aqueous dispersions. The oriented aggregation of the dry hydrate should have occurred early during industrial production. Note that precipitation of dissolved $Ca(OH)_2$ should occur upon drying. Such delayed precipitation may have contributed to either particle agglomeration (cementing action) or further crystallization of $Ca(OH)_2$ particles (e.g., autoepitaxy) and/or growth of existing ones. The latter seems more plausible, since FESEM and TEM observations (see below) did not show the presence of cement binding the particles. In any case, the latter effect appears to be negligible due to the low solubility of $Ca(OH)_2$ and the high ϕ of the putties.

TEM observations provide a more detailed insight into the nanostructure of the individual $Ca(OH)_2$ particles and clusters. Figure 4a shows a low-magnification image of typical $Ca(OH)_2$ clusters in freeze-dried slaked lime. The clusters' size ranges from a few hundred nanometers up to a few micrometers. These observations are not fully consistent with PSD results. The latter technique indicates the presence of larger aggregates, not observed with the TEM. Apparently, large clusters (of a few tens of micrometers) are not observed with the TEM because they do not tend to stick to the carbon-coated copper grids used for TEM sample preparation. Thus, the PSD analysis seems to be more accurate for quantifying larger aggregates. However, particles with size <400 nm are not quantified by the former technique. The TEM is more discriminating in the case of submicrometer particles and clusters. Figure 4b depicts one of these clusters. It is formed by a disoriented aggregate (see the ringlike SAED pattern in Figure 4b, inset) of several platelike nanocrystals with length ranging from 40 to 60 nm (measured along ⟨100⟩ direction) and a thickness of 10−30 nm (measured along [001] direction). Note that *hkl* values indicated in SAED patterns are those corresponding to the portlandite structure with space group $P\bar{3}m_1$, $a = 3.593$ Å, $c = 4.909$ Å.[53] Such disoriented $Ca(OH)_2$ aggregates, producing ringlike SAED patterns, have been observed earlier and are typically found in cement slurries of high water/cement (w/c) ratios.[54] Scarce aggregates of a few up to multiples of 10 nanocrystals showed a crystallographic orientation as indicated by SAED (Figure 4c). Scarce, larger (ca. 0.2

(53) Henderson, D. M.; Gutovsky, H. S. *Bull. Geol. Soc. Am.* **1956**, *67*, 1705.

(54) Grudemo, Å. In *Proceedings of the Fourth International Symposium on the Chemistry of Cement;* United States Standards Bureau: Washington, DC, 1960; No. 43, p 615.

μm in length) crystals were also observed, with planar, hexagonal habit (Figure 4d). Oven-dried slake lime showed significant agglomeration of numerous ($\gg$100) platelike nanoparticles, resulting in clusters with sizes up to several micrometers (Figure 5a). Such observation is consistent with PSD of oven-dried and redispersed lime putties. Although nonoriented aggregates were dominant, numerous crystallographically oriented aggregates were observed (Figure 5b). Furthermore, dominantly nonoriented aggregates often included areas with oriented clusters (Figure 5c). Early TEM−SAED studies have shown similar features in $Ca(OH)_2$ crystals formed in portland cement pastes.[55] The industrial dry hydrate showed numerous compact clusters of submicron particles (Figure 6a). Cluster size ranged from a few up to tens of micrometers. Many aggregates displayed preferred crystallographic orientation of the constituent nanoparticles (Figure 6b). Overall, little differences were observed when comparing oven-dried slaked lime and industrial dry hydrate samples. In both oven-dried slaked lime and commercial dry hydrate samples, HRTEM images showed the presence of crystallites with a thickness of 10−20 nm (measured along [001]) making up larger crystals and aggregates (Figure 7). Both disoriented (Figure 7a) and oriented (Figure 7b) aggregates were observed. Crystallites were crystallographically oriented either along ⟨100⟩ or equivalent ⟨110⟩ or along [001]. In most cases, however, some mismatching existed between nearby crystallites within an aggregate (resembling a mosaic crystal). Both SAED analyses and the latter HRTEM observations suggest that oriented-aggregation contributes to particle agglomeration.

Comparison of freeze-dried and oven-dried slaked lime samples indicates that oriented aggregation operates both before and during drying. In the first case, oriented aggregation is very limited, while randomly oriented aggregation is dominant. In the second case, it appears that drying triggers oriented aggregation. This is indicated by the large amount of aggregates with preferred crystallographic orientation in both the oven-dried slaked lime putty and the commercial dry hydrate.

XRD crystallite size measurements (Table 1) are consistent with TEM observations. Average crystallite size is ~60 nm, measured along the ⟨100⟩ (or equivalent ⟨110⟩) direction. Average particle thickness measured along the [001] direction is ~25 nm. XRD measurements do not show significant differences in crystallite size among the different $Ca(OH)_2$ types tested (both oven-dried and freeze-dried). Nonetheless, slightly smaller crystallite sizes were observed in the case of the original dry hydrate. This seems to be due to the higher nucleation rate achieved during the industrial hydration of lime, if compared with a traditional slaking process.[56] This initial effect, which could be beneficial (smaller particles would be more reactive) is counterbalanced by the subsequent drying, which leads to particle agglomeration. In fact, calculated D_{BET}/D_{hkl} values of slaked lime putty are consistently smaller than those of the dry hydrate, and they increase upon drying (Table 1). D_{BET} values range from 144 μm (freeze-dried slaked lime) up to 206 μm (dry hydrate, dispersed and dried). Such values are higher than those calculated from XRD: the highest measured D_{100} value is 63 nm. The theoretical SSA of particles with such D_{100} value is 64 m^2/g. This SSA value is more than 2 (freeze-dried slaked lime) or 3 times higher (dry hydrate) than those determined from N_2 adsorption. These results suggest that agglomeration of primary particles occurs before drying and is promoted upon drying.

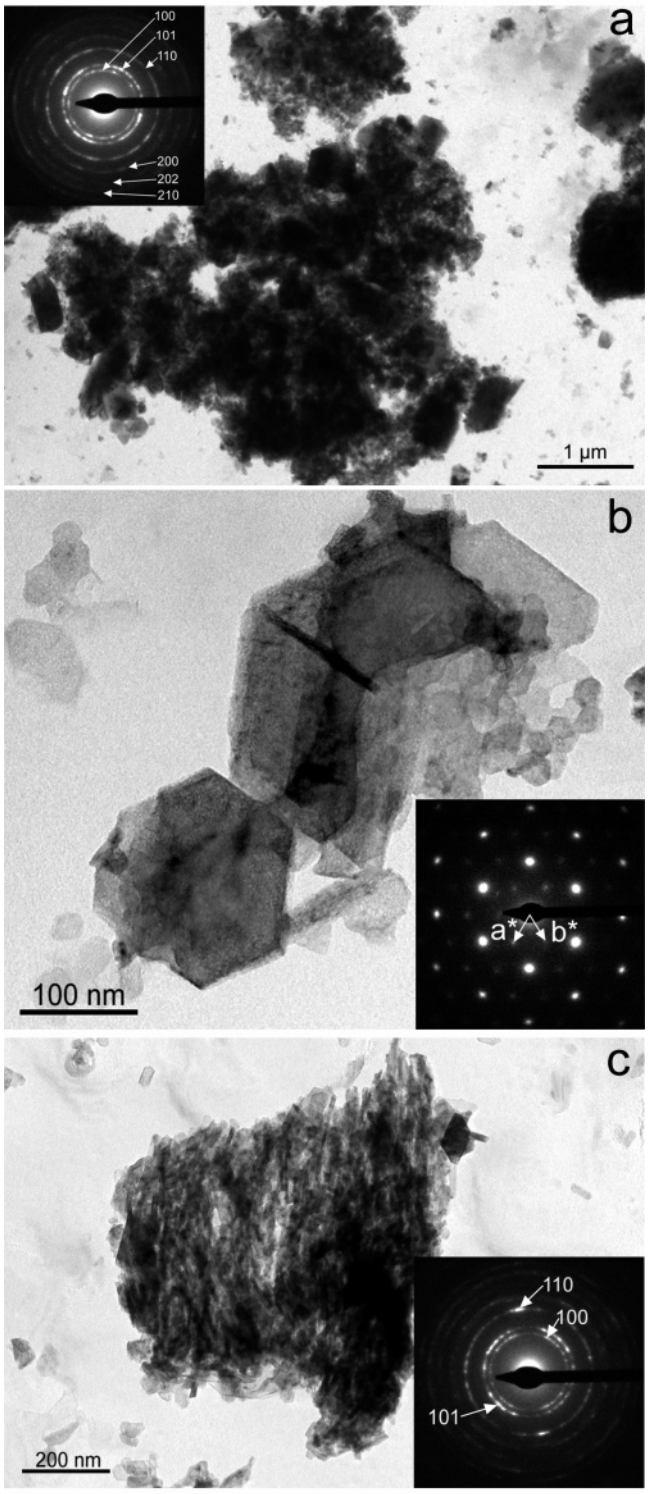

Figure 5. TEM photomicrographs of oven-dried slaked lime: (a) a typical aggregate of numerous nanoparticles. SAED (inset) demonstrates it is predominantly nonoriented (*hkl* values of diffraction rings are indicated). (b) detail of an oriented aggregate. The aggregate is oriented along ⟨100⟩ direction, thus displaying the [001] zone axis SAED pattern (inset, the a^* and b^* reciprocal axes are indicated), similar to that of a single crystal. (c) Large cluster displaying nonoriented as well as oriented aggregation via attachment by (0001) planes (which are normal to the image plane), as confirmed by the higher intensity of the discrete 110 SAED spots (inset).

(55) Groves, G. W. *Cement Concrete Res*. **1981**, *11*, 713.
(56) Hedin, R. *Plasticity of Lime Mortars*; National Lime Association: Washington, DC, 1963.

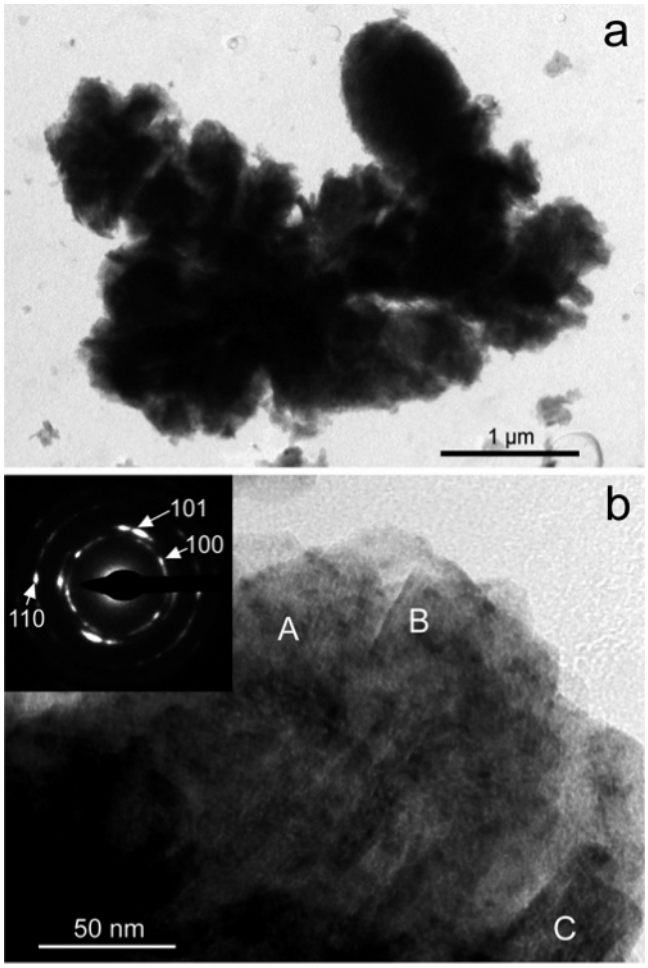

Figure 6. TEM photomicrographs of commercial dry hydrate: (a) typical micron-sized compact aggregate and (b) detail of the edge of a large oriented aggregate. Crystals aggregate along the (0001) planes (which are normal to the image plane), as demonstrated by the SAED pattern (inset). Note the slight misalignment among crystals A, B, and C, which resulted in discrete ellipsoidal SAED spots.

Overall, XRD results and agglomeration degree calculations, as well as PSD and electron microscopy analyses, show that changes in particle size undergone upon drying involve both the aggregation of primary nanocrystals with size ≤60 nm and the aggregation of larger clusters.

III.4. Aggregation of Colloidal $Ca(OH)_2$ Particles. The aggregation of colloidal particles is a phenomenon that underlies many physical, chemical, and biological processes.[57] Our results show that aggregation occurs in $Ca(OH)_2$ dispersions. The aggregates are compact, porous, and polydisperse, an observation consistent with previous TEM studies of calcium hydroxide.[58] Our data show that aggregation in $Ca(OH)_2$ dispersions operates both before and during drying, and it is more extensive in the latter case due to the subsequent increase in ϕ.[28] Our observations also indicate that a significant amount of clusters disaggregate upon redispersion. However, a fraction of the clusters does not. Such an effect can be explained by a close examination of FESEM and, particularly, TEM–SAED results. These analyses disclose a peculiar variation in the aggregation process, namely oriented aggregation/attachement of colloidal particles.[34] The oriented aggregation of $Ca(OH)_2$ colloidal particles appears to be the key to understanding the observed irreversible aggregation triggered by drying.

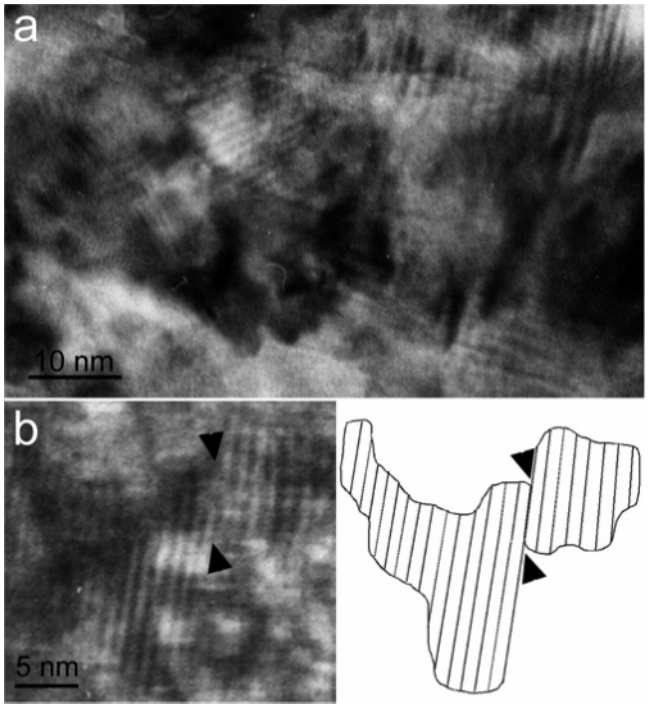

Figure 7. HRTEM micrographs of an aggregate showing lattice fringes corresponding to the (0001) planes of both (a) nonoriented and (b) oriented nanocrystals in dried slaked lime. The pair of arrows in part b indicates the contact between two oriented particles (see scheme on the right depicting lattice fringes of the two nanocrystals). The observed d-spacing of the (0001) lattice fringes is 0.98 nm, which is double the d_{001}-spacing (0.49 nm) and indicates that $Ca(OH)_2$ forms a two-layer polytype.

Oriented aggregation of nanoparticles has been recently proposed as an alternative mechanism to Ostwald ripening (i.e., growth of the larger crystals at the expense of the smaller). It has been described in a number of colloidal systems both in nature[59] and in the laboratory.[34–37,60–63] Interestingly, Yu et al.[52] have recently observed such an aggregation mechanism in $Mg(OH)_2$, which is isostructural with $Ca(OH)_2$. Spontaneous oriented aggregation operates as follows: nanometer-sized nuclei/crystals form, stereochemically attach, and aggregate, so that they share a common crystallographic orientation.[34] Oriented self-assembly of nanocrystals includes particle rotation and removal of pairs of surfaces following attachment. Attachment of randomly jiggling particles (Brownian motion) is more likely when collisions occur at equally oriented faces. Particle–particle interface now reaches its lowest energy configuration,[59] since bonding between particles removes the surface energy associated with unsatisfied bonds.[34] A strong (crystallographically coherent) bond among colloidal particles is thus established that contributes to irreversible aggregation and coarsening.

HRTEM images clearly show that nanometer-sized crystals attach, some of them in an oriented fashion while others do so in a disoriented way. However, a perfect

(57) Broide, M. L.; Cohen, R. *J. Colloid Interface Sci.* **1992**, *153*, 493.
(58) Bhandarkar, S.; Brown, R.; Estrin, J. *J. Crystal Growth* **1989**, *98*, 843.
(59) Banfield, J. F.; Welch, S. A.; Zhang, H. Z.; Ebert, T. T.; Penn, R. L. *Science* **2000**, *289*, 751.
(60) Cölfen, H.; Mann, S. *Angew. Chem., Int. Ed.* **2003**, *42*, 2350.
(61) Huang, F.; Zhang, H.; Banfield, J. F. *J. Phys. Chem. B* **2003**, *107*, 10470.
(62) Oliveira, A. P. A.; Hochepied, J. F.; Grillon, F.; Berger, M. H. *Chem. Mater.* **2003**, *15*, 3202.
(63) He, T.; Chen, D.; Jiao, X. *Chem. Mater.* **2004**, *16*, 737.

crystallographic matching does not always occur following oriented attachment: we observed some mismatching among attached particles. Such mismatching has been observed in a range of systems displaying oriented aggregation, and it leads to defect generation.[34] On the other hand, TEM low-resolution images and SAED patterns show crystallographic matching among nearby $Ca(OH)_2$ crystals in a number of aggregates. All these observations confirm that oriented aggregation is playing a significant role in our system. The fact that oriented aggregates are more abundant in both slaked lime putty samples that have undergone drying and commercial dry hydrate samples than in freeze-dried slaked lime putty samples corroborates that this aggregation mechanism is triggered by (standard) drying and is responsible for the irreversible colloidal nature of $Ca(OH)_2$ dispersions.

IV. Implications of Colloidal $Ca(OH)_2$ Aggregation in Architectural Conservation

Mortars and plasters prepared using hydrated lime as a binder set and harden via atmospheric CO_2 uptake and $CaCO_3$ formation.[10] The end product of this carbonation process regains (to a certain extent) the hardness and superior mechanical properties of the original limestone rock used to prepare quicklime (CaO). The latter is obtained by calcining limestone at 800−900 °C.[1] Hydrated lime has been a primary building material since 10 000 B.C.[15,16] The discovery of portland cement early in the 19th century led to a decline in lime mortars and plaster usage. Nonetheless, in the field of cultural heritage conservation, ordinary portland cement (OPC) has been found to be, in many applications, highly incompatible with historic lime mortar masonry when used as a replacement or repair material.[26,64] Differences in strength (excessive) and porosity (minimal) of the cement, in comparison with the lime mortar, among others, such as deleterious salts (e.g., sulfates) associated with OPC applications, has led to the general rejection of portland cement in architectural conservation.[32] In addition to historic reasons or aesthetic advantages, the use of lime mortars in conservation has been found to eliminate many of the problems associated with the recent use of portland cement:[26] (a) lime mortars do not release soluble salts; (b) they are more chemically, structurally and mechanically compatible with much ancient masonry; (c) to a certain extent, they are more able to yield under mechanical stress;[65] and (d) they undergo self-healing (related to $CaCO_3$ dissolution/reprecipitation) when fractures develop, thus increasing the structural stability of a building over time. This has led to a revival in the use of lime binders for architectural conservation purposes.[10,25,64] However, the use of "traditionally" produced slaked lime putty is often specified in preference to the use of putties made from dry hydrated lime in the restoration and conservation of historic structures with little exact technical information regarding the differences between the two materials. The preference for lime putty is based primarily upon the empirical observation of practitioners and skilled craftsmen or written historical accounts.

In this context, the irreversible aggregation associated with drying of either slaked lime putty or the industrial process resulting in the formation of dry hydrate lime is detrimental to the colloidal behavior of $Ca(OH)_2$. It strongly affects the rheological properties of hydrated lime putty and the resulting mortar/plaster performance. In particular, it affects the plasticity of lime putties.[19,20,32] Plasticity defines the most important property of a binder in the fresh state and has a decisive effect on its emplacement and ultimate performance.[22] Plasticity is strongly dependent on the abundance of colloidal (submicrometer) tabular-shaped $Ca(OH)_2$ particles.[26,56] Platelike $Ca(OH)_2$ nanoparticles have a great capacity to adsorb water (which acts as a lubricating film) and to displace easily in relation to one another without being immediately segregated.[56] This may account for the reported increase in plasticity, water retention, and workability of lime-putty-based mortars and plasters.[1,20,64,66,67] Viscosity, which directly relates to lime putty plasticity/workability, is affected by drying-related particle aggregation/coarsening. For an equal mass fraction, a putty with larger particles will be less viscous than one with smaller particles.[22,68] Irreversible aggregation occurring during drying limits the capacity of $Ca(OH)_2$ particles to adsorb water and decreases viscosity and plasticity, thus being highly detrimental when a plastic binder is desired for mason/conservation purposes.

V. Conclusions

Particle aggregation and coarsening occurs upon drying of traditionally slaked lime putty. This effect takes place early during industrial production of dry hydrated lime. The aggregation results in porous, micrometer-size aggregates. Most aggregates are formed by randomly oriented nanometer-sized platelike $Ca(OH)_2$ particles. Aggregation operates in the stable $Ca(OH)_2$ dispersion (i.e., lime putty). However, aggregation is enhanced during drying. A peculiar variation in the aggregation process is detected, namely, oriented aggregation of nanoparticles, which is also triggered during drying. While randomly oriented aggregation appears to be reversible (i.e., clusters disaggregate following redispersion in water), oriented aggregation is irreversible (i.e., the coherent structural—crystallographic—bonding among nanoparticles forming a cluster is not broken upon redispersion). The latter effect explains why industrial dry hydrate lime or dried traditional slaked lime experiences a significant and irreversible particle aggregation, which results in an increase of particle size and a reduction in surface area. Besides their impact on hydrated lime reactivity, such effects are detrimental for many applications of lime putty as a binder in lime mortars and plasters. Slaked lime putty preserves its colloidal behavior and the benefits it brings about, including the ability to "age" or undergo further modifications with time when stored as a putty.[32] The common assumption that a putty prepared with a dry hydrate will achieve many of the high mason qualities (i.e., high workability, high sand-carrying capacity, good setting and strength development, and superior durability) of traditionally slaked lime putty appears to be groundless. This information increases the ability of the architectural conservator to make the appropriate choice of repair or replacement materials.

Acknowledgment. This work has been financially supported by the Getty Conservation Institute's "Lime

(64) Ashurst, J. In *Conservation of Building and Decorative Stone*; Ashurst, J., Dimes, F. G., Eds.; Butterwoth-Heinemann: London, 1990; Chapter 4.

(65) van Balen, K.; Hayen, R.; van Gemert, D. *2005 International Building Lime Symposium Proceedings;* National Lime Association: Washington, DC, 2005.

(66) National Lime Association. *Lath Plaster* **1966**, *9*, 1.

(67) Abell, A. B.; Nichols, J. B. *ASTM Spec. Tech. Publ.* **2002**, *1432*, 23.

(68) Thomson, M. L. In *Proceedings of the International RILEM Workshop on Historic Mortars: Characterization and Tests*; Barton, P., Groot, C., Hughes, J. J., Eds.; RILEM Publication: Paris, 2000; p 163.

Mortars and Plaster" project, the Dirección General de Investigación, MCYT (Spain) under contract MAT2003-02723, and the Junta de Andalucía Research Group RNM-179. We thank the personnel of the Centro de Instrumentación Científica of the Universidad de Granada for their help during FESEM and TEM analyses. We also thank C.A. Prieto Velasco and A. Fernández Arteaga from the Department Ingeniería Química, Universidad de Granada, for their assistance during freeze-drying and PSD analysis, and N. Gálvez from the Department Química Inorgánica, Universidad de Granada, for her assistance during kinetic stability measurements. Comments and suggestions by four anonymous referees are greatly acknowledged.

LA051338F